



Article

Cite this article: Hosmann SL, Fabbri SC, Buechi MW, Hilbe M, Bauder A, Anselmetti FS (2024). Exploring beneath the retreating ice: swath bathymetry reveals sub- to proglacial processes and longevity of future alpine glacial lakes. *Annals of Glaciology* **65**, e21, 1–6. <https://doi.org/10.1017/aog.2024.18>

Received: 8 January 2024

Revised: 15 March 2024

Accepted: 9 April 2024

Keywords:

glacial geology; glacial geomorphology; glacial tills; subglacial processes

Corresponding author:

Siro L. Hosmann;

Email: siro.hosmann@unibe.ch

Exploring beneath the retreating ice: swath bathymetry reveals sub- to proglacial processes and longevity of future alpine glacial lakes

Siro L. Hosmann¹ , Stefano C. Fabbri^{1,2,3} , Marius W. Buechi¹, Michael Hilbe¹, Andreas Bauder^{4,5} and Flavio S. Anselmetti¹

¹Institute of Geological Sciences and Oeschger Centre for Climate Change Research, University of Bern, Baltzerstr. 1+3, CH-3012 Bern, Switzerland; ²Laboratoire EDYTEM, Université Savoie Mont Blanc, 5 bd de la mer Caspienne, F-73376 Le Bourget du Lac cedex, France; ³Institut des sciences de la mer de Rimouski (ISMER), Université du Québec à Rimouski and GEOTOP, 310 Allée des Ursulines, QC G5L 2Z9, Rimouski, Canada; ⁴Versuchsanstalt für Wasserbau, Hydrologie und Glaziologie (VAW), ETH Zürich, Switzerland and ⁵Swiss Federal Institute for Forest, Snow and Landscape Research (WSL), Birmensdorf, Switzerland

Abstract

Knowledge of how glaciations formed landscapes is particularly important as receding glaciers currently uncover subglacial landscapes that are prone to a series of natural hazards, but that also bring opportunities for hydropower or water resources. We present high-resolution (1×1 m) swath bathymetric data of a proglacial lake in front of the Rhonegletscher (Swiss Alps) that started to form in the early 2000s allowing a look into a freshly uncovered glacier bed and its characterized morphology in an overdeepened setting. The comparison of two surveys from 2015 and 2021 allows an unprecedented quantification of the accumulation and erosion processes in the central lake basin. This highly dynamic environment is characterized by iceberg calving, fluctuating outflow conduits, rapid sedimentation due to particle-laden meltwaters and dumped glacial debris. Assuming constant sediment yield, the Rhone Lake would persist for ~300 years. However, as intense glacier retreat continues in the coming decades, a chain of overdeepened lakes will be revealed that will act as long persisting sediment traps.

Introduction

The occurrence of subglacial basins below fluvial base level, known as overdeepenings, is widely observed but the understanding of their formation process is limited (Hooke, 1991; Preusser and others, 2010; Cook and Swift, 2012; Buechi and others, 2017; Alley and others, 2019). As glaciers strongly recede in the currently warming climate, many basins will be revealed in the coming years, resulting in a significant increase in high-alpine proglacial lakes (Linsbauer and others, 2012; Haeblerli and others, 2016, 2017; Grab and others, 2021). These newly formed lakes usually persist for many decades and sedimentary supply will alter them in the future (Geilhausen and others, 2013). A better understanding of where, how and when overdeepenings form, and how long their lacustrine state persists, can provide critical data for upcoming challenges, as it helps for hazard assessments related to processes such as ice-/rockfalls, impulse waves or glacial lake outburst floods in mountain regions (Allen and others, 2022), for long-term erosion predictions (in relation to underground storage of radioactive waste deposits; Preusser and others, 2010), hydropower management (Schaeffli and Kavetski, 2017; Delaney and others, 2018) or for contemporary ice mass dynamics (Cook and Swift, 2012). Sediment–landform associations of former glacier beds exposed during glacier retreat are prime records to study subglacial processes, which are otherwise inherently difficult to observe below the ice (Evans and others, 2006). Freshly deglaciated overdeepened basins are therefore highly instructive to better understand the subglacial morphology and related processes. Furthermore, recent studies (King and others, 2018; Zhang and others, 2023) reported that lake-terminating glaciers in the greater Himalaya experience more negative mass balance compared to land-terminating glaciers and that this difference is further amplified when subaqueous ice mass loss is considered. They show a significant correlation between the subaqueous mass loss and the presence of a lake-glacier contact suggesting that proglacial lakes accelerate the loss due to increased melt at the interface. Additionally, the size and depth of these lakes are important factors that control the mechanisms involved in the rate of dynamical glacier thinning and ice calving (Pronk and others, 2021), highlighting the importance of quantifying deglaciation processes in an overdeepened setting. However, so far very little data have been acquired from freshly exposed overdeepened lakes, as water prevents easy access.

With this study, we provide a 3-D view of a submerged and calving glacier front in a high-alpine setting. This allows imaging of the submerged ice-sediment interface and quantification of ongoing subglacial processes interacting with the lake at unprecedented resolution. With a time-lapse swath-bathymetric recording of this freshly exposed subglacial

overdeepening, we gain new insights into the submerged morphological features and the role and rates of glacial processes that are occurring during the recession of the ice mass. Furthermore, we precisely map and quantify the change in sediment infill in the proglacial basin over a 6-year period. This allows us to get a detailed insight of (i) the pace at which this highly dynamic environment changes, (ii) how much and what type of sediment is emplaced at which location in the overdeepened basin and (iii) what potential implications arise for other proglacial lakes globally that are in a similar phase of rapid growth.

Setting

The Rhone Lake, embedded in the Grimsel granodiorite rocks of the Aar Massif (Abrecht, 1994), is a proglacial lake at 2208 m.a.s.l. currently in contact with the front of the Rhonegletscher and the source of the River Rhone, located in the Central Alps in Switzerland (Fig. 1a). The lake started to form ~20 years ago and covered an area of ~0.46 km² in September 2021; however, it is growing continuously due to glacier recession. During the peak of the Little Ice Age (~1870 CE), the Rhonegletscher reached almost to the settlement of Gletsch, ~2.5 km downstream of the current glacier tongue (Fig. 1a). The most recent sub- and englacial drainage system of the

Rhonegletscher terminus is well-known from ground-penetrating radar data (Church and others, 2019).

Data acquisition

A Kongsberg EM2040 multibeam echosounder (mounted in front of a 3 m × 4 m platform) with a 300 kHz operating frequency (technical details in Hilbe and Anselmetti, 2014; Fabbri and others, 2021) was used during two surveys in October 2015 and September 2021, yielding a 1 × 1 m high-resolution swath bathymetry grid. Three short cores were obtained with a Uwitec USC 06000 gravity corer. Two core locations (RH21_1A and RH21_1B) are situated in the inflow area (II in Fig. 1c) and one (RH21_4) in the terrace area (IV in Fig. 1c; see Supplementary material).

High-resolution bathymetric data

The high-resolution swath bathymetry map of the Rhone Lake (Figs 1b and S1) shows the overall overdeepened basin (with a depth of at least 38 m) and its internal relief upstream of the southern bedrock ridge. Four main geomorphic areas can be distinguished: (I) the central basin, separated by a moraine (formed in 2014), (II) the currently active glacial inflow area with the submerged ice front (Figs 2 and 3), (III) the upper

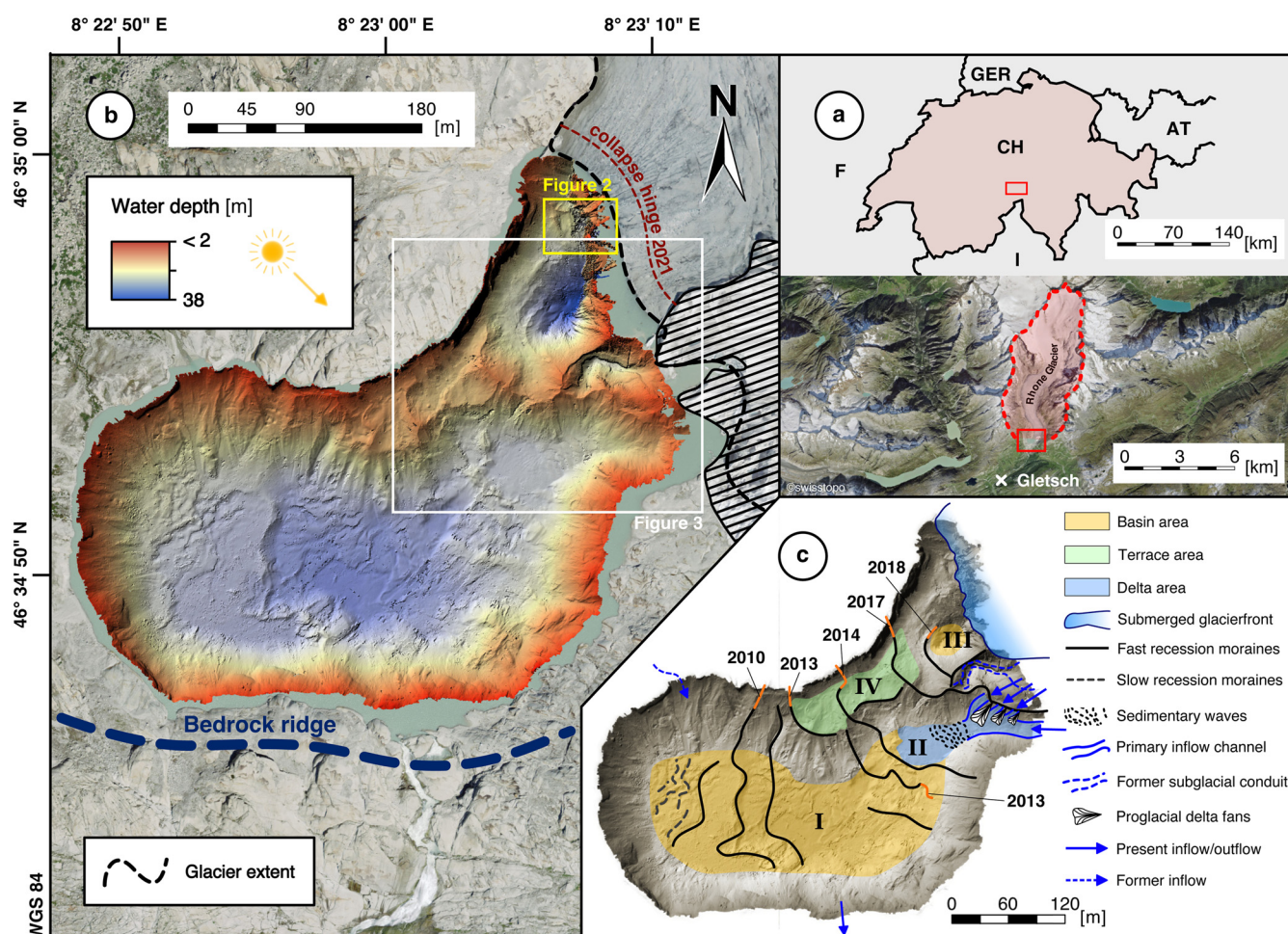


Figure 1. (a) Location of the catchment area in the Central Swiss Alps. (b) High-resolution bathymetric map of Rhone Lake recorded in 2021. Background map by swisstopo. Glacier extent marked by black dashed line. Striped area in the east indicates glacier covered by white blankets to prevent ice melting preserving a touristic ice cave. (c) Morphological interpretation of the bathymetric dataset from 2021.

proximal basin and (IV) the terrace area. The laterally continuous, back-stepping sequence of arcuate subaqueous moraines in the central basin (black lines with its approximated formation year in Fig. 1c) marks former grounding lines of the glacier. Considering that the initial lake formed only ~20 years ago, eight ‘mini-moraines’ with heights up to 2 m and widths of up to 5 m formed between 2009 and 2021 CE and symbolize the rate of the recession that is comparable to annual retreat moraines mapped in deglaciating fjords on Svalbard (Ottesen and Dowdeswell, 2006). The moraine-crest elevations also strongly influence the sediment distribution within the basin: the delimiting ridge, built after 2017 CE (GLAMOS, 2022, Fig. S2), separates the central basin (I) from the younger upper proximal basin (III). Consequently, the dividing character of this ridge directs the current inflow channel to the south and creates a new subaquatic delta channel, which leads to an inflow area (II) with all elements of a modern delta (Fig. 3). However, occasional sediment overspill towards the south across the moraine ridge is confirmed by outflow channels and sediment waves south of the ridge.

Discussion: glacial and proglacial processes

Subglacial bedrock erosion

Initial formation of the overdeepened bedrock basins is tied to subglacial erosion. The traces of bedrock abrasion and plucking are abundantly exposed around the lake (Alley and others, 2019). The central basin (I) and the upper proximal area (III) are separated by the prominent SE-NW trending ridge formed in 2017 CE (Figs 1c and 2), which possibly is composed of an underlying bedrock high that is topped by moraine sediments. The central and the upper basins are thus mainly controlled by the selective bedrock erosion of the glacier (Church and others, 2018). The south-western ice-flow direction features a steeper flank to the central basin (I), and a less steep slope to the freshly revealed basin (III). The main shaping process was glacial bedrock

erosion, leading to the separation of the two basins, where after the lake morphology became additionally accentuated by glaciogenic sedimentation.

Ice-front morphology and meltwater outlets

The point cloud of the ungridded multibeam data (Fig. 2a, see Fig. S3 for cross-sections) allows novel perspectives of a submerged glacier front. The lake floor follows the subglacial topography into a new and deeper basin, which is currently still covered with ice (Church and others, 2018). The glacier front forms a submerged part, overhanging the ice-sediment contact by 5 m (Fig. 2a). On 9 September 2021, this entire submerged part of the glacier front with a volume of $200\,000 \pm 20\,000\text{ m}^3$ (Malt, 2023) broke completely off (see Fig. 1b for collapse hinge) during a calving event, highlighting its limited stability. Formation of similar submerged ice masses is known from terminal glacier lakes in New Zealand, where their formation under stable water levels is linked to preferential melting by warm lake-surface waters (Robertson and others, 2012; Purdie and others, 2016).

Glaciers terminating in overdeepenings are known to comprise a multitude of seasonally variable drainage systems using sub- and englacial pathways (Swift and others, 2021). At the Rhonegletscher terminus, the activity of englacial channels has been well-documented (Church and others, 2019). A ~20 m deep, 9 m wide and ~90 m long meandering channel (Fig. 3) is visible upstream of the location of the 2017 CE glacial front. This channel has a reversed slope profile, i.e. the channel base rises in downstream direction, characteristic for terminal overdeepenings (Swift and others, 2005). Crossing the moraine structure towards the south at the former exit of the subglacial conduit, the outflow channel feeds into a high-backscatter-intensity area interpreted as subglacial outflow channel descending into the central basin (Fig. 3). The coarse sediment contributed to the formation of the 2017 CE subaquatic moraine ridge and reflects the dynamic processes with high particle supply at the former ice front during retreat.

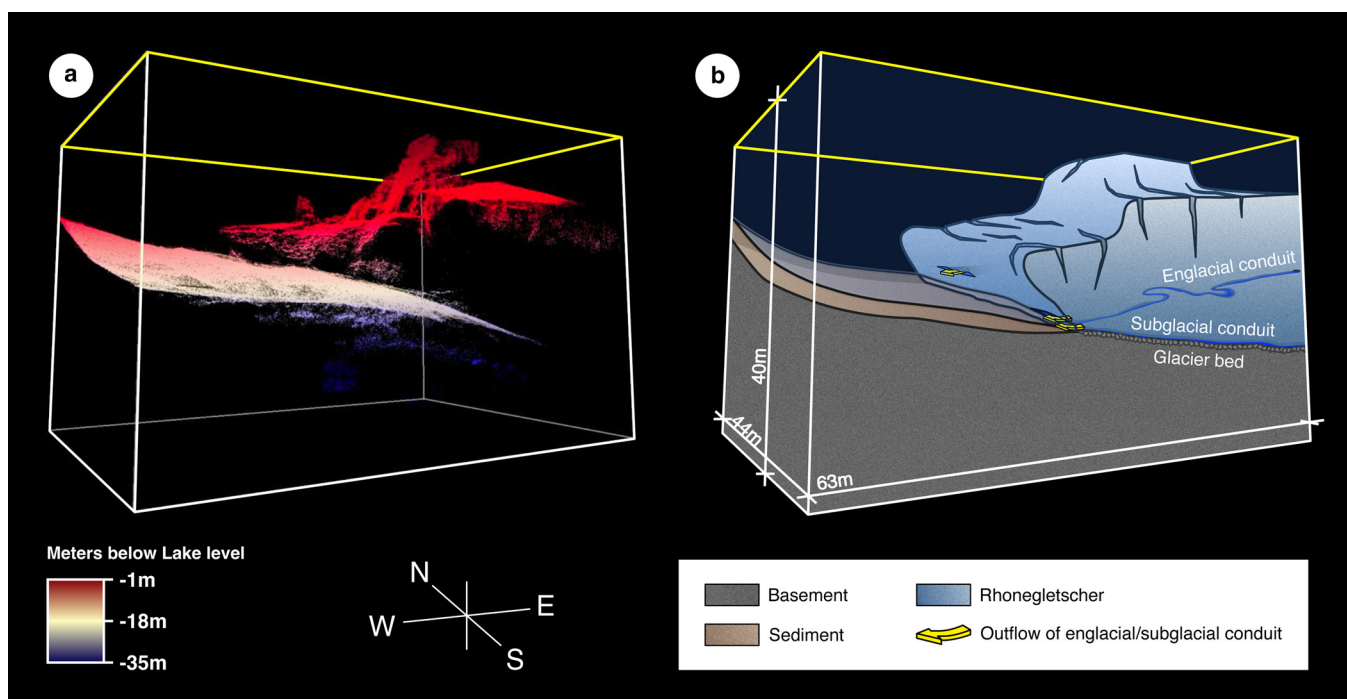


Figure 2. (a) Ungridded point cloud of swath-bathymetry data of the submerged glacier front. (b) 3-D interpretation of the data in figure (a). Model shows morphological features contributing to the formation of a subglacial overdeepening.

Glacigenic sedimentation

The variable spacing of the subaquatic moraines likely reflects a combination of changes in the rate of recession across the basin and the efficiency of moraine formation. As the interface between the glacier front and the lake bottom and also the resulting location of the subaquatic moraine is very complex, the interpreted

cores taken in this area show differences in grain size with thinner layers of very fine-grained sediment intercalated by more sandy and thicker layers (Fig. S4). These lacustrine sediments indicate that deposition started immediately after deglaciation, contrasting other studies that identified a potential lag in similar settings most likely related to inherited glacial topography and respective coring location (Piret and Bertrand, 2022).

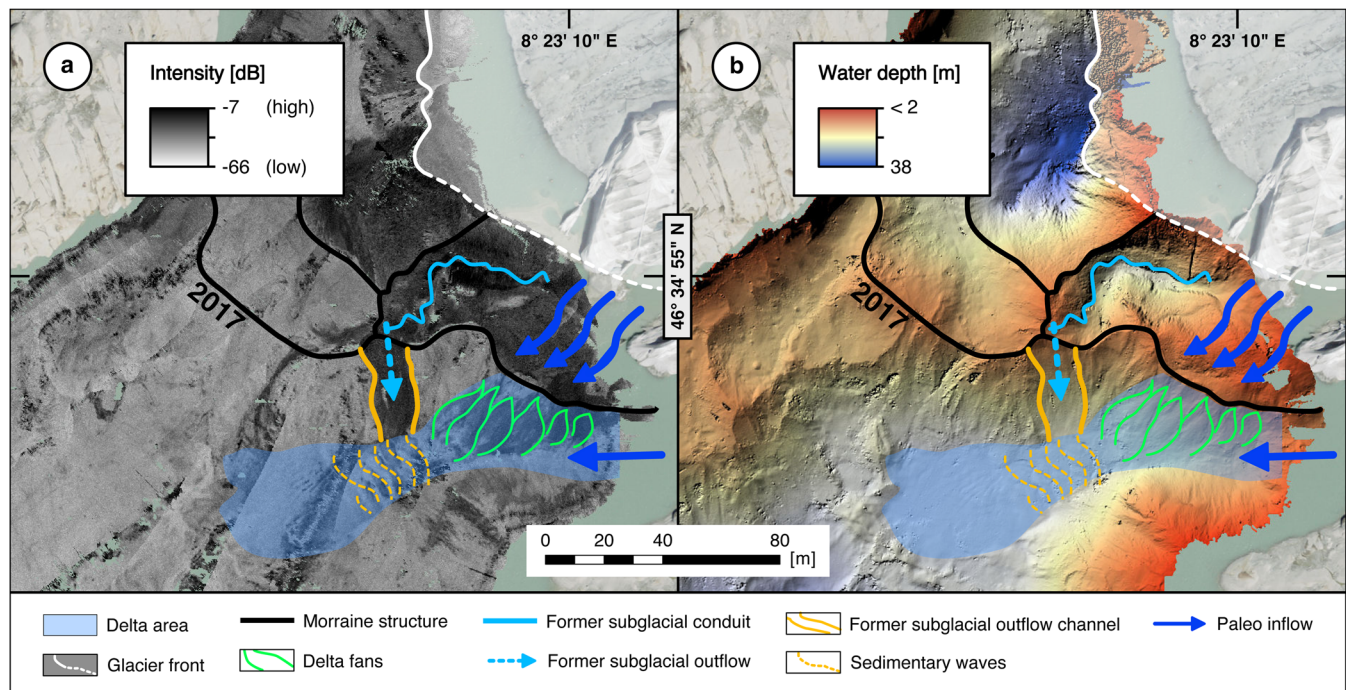


Figure 3. (a) Backscatter-intensity map with interpretation (darker areas indicate more coarse-grained sediment or harder ground) and (b) bathymetric map of same area. Full coverage of the backscatter-intensity map is shown in Figure S1.

years when moraines formed are somehow an approximation (Figs 1c and S2). The narrow spacing indicates a slow retreat from ~2000 until 2010 CE, when only small, slow recessional moraines were formed (Fig. 1c). After 2010 CE, the new main discharge opened up, melting and retreat accelerated producing larger and more widely spaced moraines, especially in the deepest part, that formed on average every 2 years. Pronounced winter readvances may have further contributed to bulldozing and thrusting of these sediments at the grounding line leading to even more pronounced ridges as known from nearby terrestrial valley-glacier settings (Lukas, 2012). Although the building of moraines are influenced by different factors (Barr and Lovell, 2014), the correlation between the mass balance of the Rhonegletscher and the distances between biannual moraines is striking and especially notable in years with high loss in mass, such as in 2010/2011 CE, when the retreat and the spacing are large. In years with a lower mass loss, such as in 2012/2013 CE, the spacing between recessional moraines becomes smaller (GLAMOS, 1881–2023). However, this relation may be modified as very big ice mass losses can also be produced by calving events such as in 2021 CE.

Recent proglacial lacustrine sedimentation

The main delta area (II), hosting present and former inflows, supplies the central basin with sediment. The backscatter-intensity pattern (Fig. 3) shows that coarser material is located all along the front of the current glacier tongue. Two short sediment

Several geomorphologic elements relate to the modern and the former inflows. These areas are characterized by sediment waves, whose sizes depend on the flow velocity (Stow and others, 2009). In the modern inflow area, sediment-wavelength amounts to ~4 m indicating an average influx velocity of $\sim 0.4\text{--}0.8\text{ m s}^{-1}$, high enough to be erosional (Stow and others, 2009). The eastern inflow is split into northern and southern branch (Fig. 3). The eastern part of the northern shore of the central basin is also characterized by prominent sediment waves and channels reminiscent to the ones described above from the modern inflow area (Fig. 1b).

Broader impact: longevity of newly formed proglacial lakes

To calculate the sediment yield released by the Rhonegletscher, we used the 6-year sediment-thickness map (2015–2021, see Fig. S5), which shows the sediment-volume difference over this period, and extrapolated it to the 2021 position of the glacier tongue and the western shore where ice prevented a survey in 2015. To fill the data gaps, we extrapolated the rate of 16.7 cm a^{-1} for the shallow-water zone in the west and 33.33 cm a^{-1} for the area towards the glacier tongue, respectively (Fig. 4). Overall, the 6-year sediment volume deposited in Rhone Lake amounts to $\sim 120\,000\text{ m}^3$, averaging $\sim 20\,000\text{ m}^3$ per year. Corrected for sediment porosity of 35% and a particle density of 2.6 g cm^{-3} (Anselmetti and others, 2007), this equals an annual particle mass of 34.5 kt. Taking into consideration of 5.8 kt of fine suspended particles outflowing the lake every year (assuming a sediment/suspended particle ratio as in a nearby glaciated catchment;

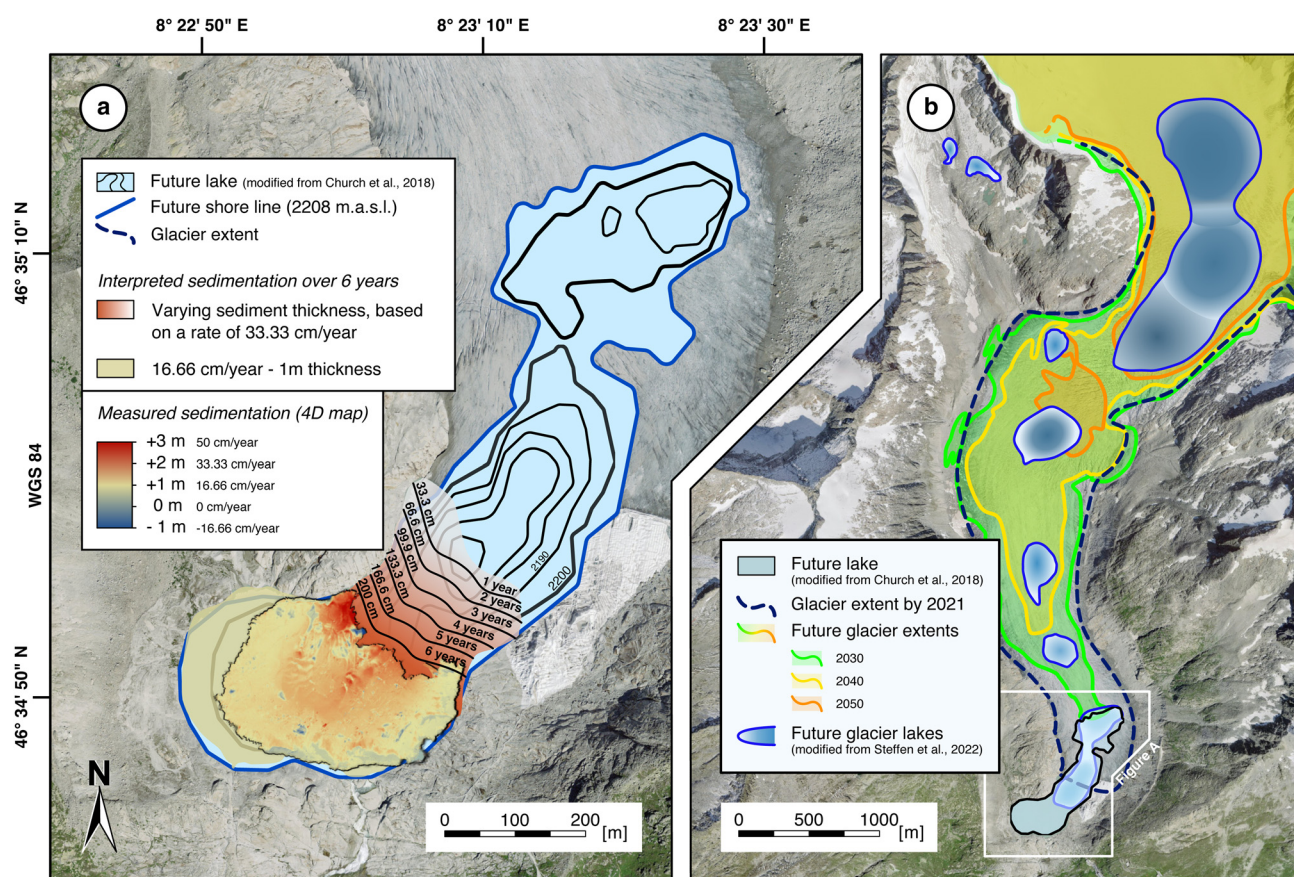


Figure 4. (a) Sediment thickness over 6 years based on two repetitive bathymetric surveys and retreating ice tongue. Future lake, modified from Church and others (2018). (b) Future proglacial lakes at the Rhonegletscher based on calculations by swisstopo.

Anselmetti and others, 2007), the total annual sediment yield amounts to 40.3 kt stemming from denudation rates of 0.6 and 1.2 mm for the complete and the glaciated catchment, respectively. To assess the future development of the Rhone Lake, we used the bedrock model of Church and others (2018) to predict the lake's outline and volume in ice-free conditions that will be reached in ~2030 (Steffen and others, 2022) (Fig. 4a). Extrapolating our sedimentation rates indicates that 294 years will be needed for the complete filling of the future lake basin. However, as accelerated Rhonegletscher retreat will form nine new overdeepened lakes within 30 years with depths up to 170 m (Steffen and others, 2022; Fig. 4b), Rhone Lake will soon be disconnected from the main particle supply as these upstream lakes will act as efficient sediment traps so that Rhone Lake as well as the future chain of lakes will survive for centuries to come. This longevity of these proglacial lakes needs to be considered for challenges such as water-resource management and lake-derived natural hazards (impulse waves from rock falls, glacial outbursts), but also provides a high potential for hydropower, water resources and tourism. As the number of such high-alpine proglacial lakes is expected to increase exponentially in the future (Linsbauer and others, 2012; Grab and others, 2021; Steffen and others, 2022), and as glacier retreat outpaces lacustrine sedimentation, the longevity of glacial lakes will also have consequences for the particle supply and hydrological regime for the downstream areas.

Supplementary material. The supplementary material for this article can be found at <https://doi.org/10.1017/aog.2024.18>.

Acknowledgements. We are grateful to the staff of the Eisgrotte allowing easy access to the lake. We thank Franziska Nyffenegger for support during the 2015 field campaign.

References

- Abrecht J (1994) Geologic units of the Aar Massif and their alpine rock associations – a critical review. *Schweizerische Mineralogische Und Petrographische Mitteilungen* 74(1), 5–27.
- Allen S and 5 others (2022) Assessment principles for glacier and permafrost hazards in mountain regions. In *Oxford Research Encyclopedia of Natural Hazard Science*. Oxford University Press, 1–72. doi: [10.1093/acrefore/9780199389407.013.356](https://doi.org/10.1093/acrefore/9780199389407.013.356)
- Alley RB, Cuffey KM and Zoet LK (2019) Glacial erosion: status and outlook. *Annals of Glaciology* 60(80), 1–13. doi: [10.1017/aog.2019.38](https://doi.org/10.1017/aog.2019.38)
- Anselmetti FS and 6 others (2007) Effects of alpine hydropower dams on particle transport and lacustrine sedimentation. *Aquatic Sciences* 69, 179–198. doi: [10.1007/s00027-007-0875-4](https://doi.org/10.1007/s00027-007-0875-4)
- Barr ID and Lovell H (2014) A review of topographic controls on moraine distribution. *Geomorphology* 226, 44–64. doi: [10.1016/j.geomorph.2014.07.030](https://doi.org/10.1016/j.geomorph.2014.07.030)
- Buechi MW, Frank SM, Graf HR, Menzies J and Anselmetti FS (2017) Subglacial emplacement of tills and meltwater deposits at the base of overdeepened bedrock troughs. *Sedimentology* 64(3), 658–685. doi: [10.1111/sed.12319](https://doi.org/10.1111/sed.12319)
- Church G and 5 others (2019) Detecting and characterising an englacial conduit network within a temperate Swiss glacier using active seismic, ground penetrating radar and borehole analysis. *Annals of Glaciology* 60(79), 193–205. doi: [10.1017/aog.2019.19](https://doi.org/10.1017/aog.2019.19)
- Church G, Bauder A, Grab M, Hellmann S and Maurer H (2018) High-resolution helicopter-borne ground penetrating radar survey to determine glacier base topography and the outlook of a proglacial lake, 17th International Conference on Ground Penetrating Radar (GPR), Rapperswil, Switzerland, June 18–21, 2018, pp. 247–252. doi: [10.1109/ICGPR.2018.8441598](https://doi.org/10.1109/ICGPR.2018.8441598)
- Cook SJ and Swift DA (2012) Subglacial basins: their origin and importance in glacial systems and landscapes. *Earth-Science Reviews* 115(4), 332–372. doi: [10.1016/j.earscirev.2012.09.009](https://doi.org/10.1016/j.earscirev.2012.09.009)
- Delaney I, Bauder A, Huss M and Weidmann Y (2018) Proglacial erosion rates and processes in a glacierized catchment in the Swiss Alps. *Earth Surface Processes and Landforms* 43(4), 765–778. doi: [10.1002/esp.4239](https://doi.org/10.1002/esp.4239)

- Evans DJA, Phillips ER, Hiemstra JF and Auton CA (2006) Subglacial till: formation, sedimentary characteristics and classification. *Earth-Science Reviews* **78**(1–2), 115–176. doi: [10.1016/j.earscirev.2006.04.001](https://doi.org/10.1016/j.earscirev.2006.04.001)
- Fabbri SC and 5 others (2021) Subaqueous geomorphology and delta dynamics of Lake Brienz (Switzerland): implications for the sediment budget in the alpine realm. *Swiss Journal of Geosciences* **114**(1), 22. doi: [10.1186/s00015-021-00399-1](https://doi.org/10.1186/s00015-021-00399-1)
- Geilhausen M, Morche D, Otto J-C and Schrott L (2013) Sediment discharge from the proglacial zone of a retreating Alpine glacier. *Zeitschrift Für Geomorphologie, Supplementary Issues*, **57**(2), 29–53. doi: [10.1127/0372-8854/2012/S-00122](https://doi.org/10.1127/0372-8854/2012/S-00122)
- GLAMOS (1881–2023) The Swiss Glaciers 1880–2022/23: Glaciological Reports No 1–142: Yearbooks of the Cryospheric Commission of the Swiss Academy of Science (SCNAT), published since 1964 by VAW/ETH Zurich. doi: [10.18752/glrep_series](https://doi.org/10.18752/glrep_series)
- GLAMOS (2022) Bauder, A., Huss, M., Linsbauer, A. (eds.), The Swiss Glaciers 2019/20 and 2020/2021: Glaciological Reports No 141/42: Yearbooks of the Cryospheric Commission (EKK) of the Swiss Academy of Science (SCNAT), published by VAW/ETH Zurich. doi: [10.18752/glrep_141-142](https://doi.org/10.18752/glrep_141-142)
- Grab M and 6 others (2021) Ice thickness distribution of all Swiss glaciers based on extended ground-penetrating radar data and glaciological modeling. *Journal of Glaciology* **67**(266), 1074–1092. doi: [10.1017/jog.2021.55](https://doi.org/10.1017/jog.2021.55)
- Haeblerli W and 5 others (2016) New lakes in deglaciating high-mountain regions – opportunities and risks. *Climatic Change* **139**(2), 201–214. doi: [10.1007/s10584-016-1771-5](https://doi.org/10.1007/s10584-016-1771-5)
- Haeblerli W, Schaub Y and Huggel C (2017) Increasing risks related to landslides from degrading permafrost into new lakes in de-glaciating mountain ranges. *Geomorphology* **293**, 405–417. doi: [10.1016/j.geomorph.2016.02.009](https://doi.org/10.1016/j.geomorph.2016.02.009)
- Hilbe M and Anselmetti FS (2014) Signatures of slope failures and river-delta collapses in a perialpine lake (Lake Lucerne, Switzerland). *Sedimentology* **61**(7), 1883–1907. doi: [10.1111/sed.12120](https://doi.org/10.1111/sed.12120)
- Hooke RL (1991) Positive feedbacks associated with erosion of glacial cirques and overdeepenings. *Geological Society of America Bulletin* **103**(8), 1104–1108. doi: [10.1130/0016-7606\(1991\)103%3C1104:PFAWEO%3E2.3.CO;2](https://doi.org/10.1130/0016-7606(1991)103%3C1104:PFAWEO%3E2.3.CO;2)
- King O, Dehecq A, Quincey D and Carrivick J (2018) Contrasting geometric and dynamic evolution of lake and land-terminating glaciers in the central Himalaya. *Global and Planetary Change* **167**, 46–60. doi: [10.1016/j.gloplacha.2018.05.006](https://doi.org/10.1016/j.gloplacha.2018.05.006)
- Linsbauer A, Paul F and Haeblerli W (2012) Modeling glacier thickness distribution and bed topography over entire mountain ranges with glabtop: application of a fast and robust approach. *Journal of Geophysical Research: Earth Surface* **117**(3), doi: [10.1029/2011JF002313](https://doi.org/10.1029/2011JF002313)
- Lukas S (2012) Processes of annual moraine formation at a temperate alpine valley glacier: insights into glacier dynamics and climatic controls. *Boreas* **41**(3), 463–480. doi: [10.1111/j.1502-3885.2011.00241.x](https://doi.org/10.1111/j.1502-3885.2011.00241.x)
- Malt V (2023) Flotation event at the tongue of Rhonegletscher, term paper ETH Zürich, 39 pp.
- Ottesen D and Dowdeswell JA (2006) Assemblages of submarine landforms produced by tidewater glaciers in Svalbard. *Journal of Geophysical Research: Earth Surface* **111**(1), 1–18. doi: [10.1029/2005JF000330](https://doi.org/10.1029/2005JF000330)
- Piret L and Bertrand S (2022) Multidecadal delay between deglaciation and formation of a proglacial lake sediment record. *Quaternary Science Reviews* **294**, 107752. doi: [10.1016/j.quascirev.2022.107752](https://doi.org/10.1016/j.quascirev.2022.107752)
- Preusser F, Reitner JM and Schlüchter C (2010) Distribution, geometry, age and origin of overdeepened valleys and basins in the Alps and their foreland. *Swiss Journal of Geosciences* **103**(3), 407–426. doi: [10.1007/s00015-010-0044-y](https://doi.org/10.1007/s00015-010-0044-y)
- Pronk JB, Bolch T, King O, Wouters B and Benn DI (2021) Contrasting surface velocities between lake- and land-terminating glaciers in the Himalayan region. *The Cryosphere* **15**(12), 5577–5599. doi: [10.5194/tc-15-5577-2021](https://doi.org/10.5194/tc-15-5577-2021)
- Purdie H, Bealing P, Tidey E, Gomez C and Harrison J (2016) Bathymetric evolution of Tasman Glacier terminal lake, New Zealand, as determined by remote surveying techniques. *Global and Planetary Change* **147**, 1–11. doi: [10.1016/j.gloplacha.2016.10.010](https://doi.org/10.1016/j.gloplacha.2016.10.010)
- Robertson CM, Benn DI, Brook MS, Fuller IC and Holt KA (2012) Subaqueous calving margin morphology at Mueller, Hooker and Tasman glaciers in Aoraki/Mount Cook National Park, New Zealand. *Journal of Glaciology* **58**(212), 1037–1046. doi: [10.3189/2012JG12J048](https://doi.org/10.3189/2012JG12J048)
- Schaeffli B and Kavetski D (2017) Bayesian spectral likelihood for hydrological parameter inference. *Water Resources Research* **53**(8), 6857–6884. doi: [10.1002/2016WR019465](https://doi.org/10.1002/2016WR019465)
- Steffen T, Huss M, Estermann E, Hodel E and Farinotti D (2022) Volume, evolution and sedimentation of future glacier lakes in Switzerland over the 21st century. *Earth Surface Dynamics* **10**(4), 723–741. doi: [10.5194/esurf-10-723-2022](https://doi.org/10.5194/esurf-10-723-2022)
- Stow DAV and 5 others (2009) Bedform-velocity matrix: the estimation of bottom current velocity from bedform observations. *Geology* **37**(4), 327–330. doi: [10.1130/G25259A.1](https://doi.org/10.1130/G25259A.1)
- Swift DA and 5 others (2021) The hydrology of glacier-bed overdeepenings: sediment transport mechanics, drainage system morphology, and geomorphological implications. *Earth Surface Processes and Landforms* **46**(11), 2264–2278. doi: [10.1002/esp.5173](https://doi.org/10.1002/esp.5173)
- Swift DA, Nienow PW, Hoey TB and Mair DWF (2005) Seasonal evolution of runoff from Haut Glacier d'Arolla, Switzerland and implications for glacial geomorphic processes. *Journal of Hydrology* **309**(1–4), 133–148. doi: [10.1016/j.jhydrol.2004.11.016](https://doi.org/10.1016/j.jhydrol.2004.11.016)
- Zhang G and 9 others (2023) Underestimated mass loss from lake-terminating glaciers in the greater Himalaya. *Nature Geoscience* **16**, 333–338. doi: [10.1038/s41561-023-01150-1](https://doi.org/10.1038/s41561-023-01150-1)